

## Full Articles

### Stabilization of [2.2]paracyclophane anion as a result of transannular interaction \*

I. V. Fedyanin, K. A. Lyssenko,\* Z. A. Starikova, and M. Yu. Antipin

A. N. Nesmeyanov Institute of Organoelement Compounds, Russian Academy of Sciences,  
28 ul. Vavilova, 119991 Moscow, Russian Federation.  
Fax: +7 (095) 135 5085; E-mail: kostya@xray.ineos.ac.ru

Topological analysis of the electron density distribution in the [2.2]paracyclophane radical anion and radical cation based on the results of B3PW91/6-31+G(d) calculations revealed that reduction of the electron affinity energy down to  $-0.5$  eV (more than a twofold decrease compared to benzene) is a result of transannular interaction between the benzene rings.

**Key words:** [2.2]paracyclophane and its radical anion and radical cation, theory "Atoms in molecules," quantum-chemical calculations, transannular interaction

Intramolecular and intermolecular interactions between aromatic systems play a great role in the formation of supramolecular structure. They are responsible for a number of physicochemical properties of these systems and can also serve as a basis for biological recognition processes.<sup>1,2</sup> Analysis of the structures retrieved from the Cambridge Structural Database (CSD) showed that in most cases intermolecular stacking interaction is accompanied by minor displacement of aromatic rings relative to each other while a perfect, "face-to-face" arrangement of the rings is rare to occur.<sup>3</sup> On the contrary, in the case of intramolecular interactions between  $\pi$ -systems this type of ring arrangement occurs quite frequently (see, *e.g.*, Refs. 2, 4).

A classical example of the molecule with forced "face-to-face" arrangement of aromatic rings is provided by [2.2]paracyclophane (**1**, Fig. 1). Based on the geometric criteria only, a strong stacking interaction must occur in

this system. According to X-ray analysis data,<sup>5</sup> the distance between the "boat" planes of two aromatic rings in unsubstituted [2.2]paracyclophane **1** is much shorter than the sum of the van der Waals radii (3.099(1) vs. 3.40 Å, respectively). However, an experimental and theoretical study of the electron density distribution function,  $\rho(\mathbf{r})$ , performed in the framework of the topological theory "Atoms in molecule" (AIM)<sup>6</sup> in the same study<sup>5</sup> revealed no attractive interaction between the ring  $\pi$ -systems both in the crystal and in isolated molecule. Similar results were also obtained for the 4,7-benzoquinone[2.2]paracyclophane molecule with nonequivalent rings.<sup>7</sup> It should be noted that in the last-mentioned molecule the rings are rotated relative to each other by 11.4° in the crystal and by 38° in the isolated molecule.

With allowance for intramolecular charge transfer<sup>8</sup> in the excited state of molecule **1** it was of interest to assess how the changes in the HOMO and LUMO energies will

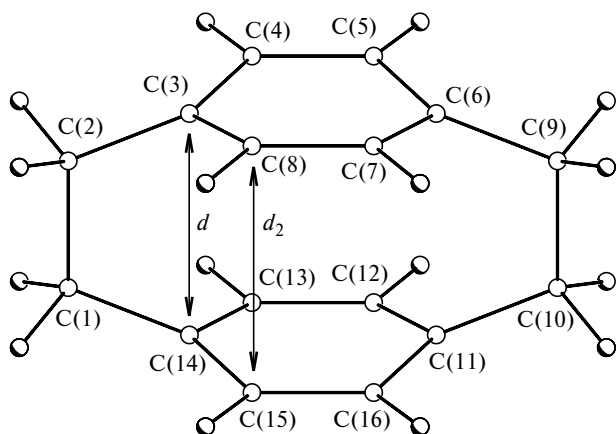


**Fig. 1.** General view of and atomic numbering scheme for the [2.2]paracyclophane molecule.

affect the character of the inter-ring intramolecular interaction. Such changes can be achieved by introducing electron-donor or electron-acceptor substituents and by changing the charge of the molecule. Formally, molecules with acceptor or donor substituents can be modelled using the [2.2]paracyclophane radical anion (**1a**) and radical cation (**1c**) as "electron-rich" or "electron-deficient" systems, respectively.

This work was carried out in a continuation of our investigations of the derivatives of compound **1**.<sup>5,7</sup> Here, we report on a quantum-chemical study of radicals **1a** and **1c**. The electron density distribution was analyzed in the framework of the AIM theory. The advantages of this theory in treating forced intramolecular interactions were demonstrated in a number of theoretical<sup>7,9</sup> and experimental studies.<sup>5,10–12</sup> Since in molecule **1** we deal with charge delocalization between two aromatic systems, one can expect a decrease in the electron affinity energy and in the first ionization potential of **1** compared to the corresponding characteristics of benzene. For comparison, we also calculated the energies of neutral benzene molecule and of the benzene anion and cation.

Quantum-chemical calculations of all the systems studied in this work were carried out using the density functional approach (UB3PW91 functional) with the 6-31+G(d) basis set and the GAUSSIAN-98 program suite.<sup>13</sup> Full geometry optimization was performed using conventional convergence criteria (0.00045 and 0.0018 a.u. for the maximum force and displacement, respectively).

When calculating open-shell systems, the problem of spin state purity poses, because the wave function is not an eigenfunction of the total electron spin operator and can therefore contain an admixture of higher multiplet states. In our calculations of the molecules containing one unpaired electron the spin state purity evaluated from the  $\langle S^2 \rangle$  magnitude deviates from an ideal value of 0.75 by at most 0.018 (2.4%, Table 1). Hence, the radicals

**Table 1.** Total energies ( $E_{\text{tot}}$ ), first ionization potentials (IP), and electron affinity energies (EA) of [2.2]paracyclophane molecule **1**, radical anion **1a**, radical cation **1c**, benzene molecule, benzene radical anion, and benzene radical cation obtained from B3PW91/6-31+G(d) calculations

System	$E_{\text{tot}}/\text{hartree}$	$\langle S^2 \rangle$	EA	IP
			eV	
<b>1</b>	–619.0850172	0	–0.50	–7.45 (–8.1) <sup>a</sup>
<b>1a</b>	–619.0668275	0.755	—	—
<b>1c</b>	–618.8100389	0.759	—	—
C <sub>6</sub> H <sub>6</sub>	–232.1666136	0	–1.34 (–1.12) <sup>b</sup>	–9.10 (–9.24) <sup>b</sup>
C <sub>6</sub> H <sub>6</sub> <sup>–</sup>	–232.1173546	0.756	—	—
C <sub>6</sub> H <sub>6</sub> <sup>+</sup>	–231.832088	0.768	—	—

<sup>a</sup> According to UV photoelectron spectroscopy data.<sup>14</sup>

<sup>b</sup> Obtained from B3LYP/DZP++ calculations.<sup>15,16</sup>

under study are characterized by small admixture of higher multiplet states.

Topological analysis of the function  $\rho(\mathbf{r})$  was performed using the AIMPAC program package<sup>17</sup> and the wave functions obtained from optimization. Since the results<sup>5</sup> for **1** were obtained with the basis set containing no diffuse functions, here we also carried out B3PW91/6-31+G(d) calculations of neutral molecule **1** to provide a correct comparison of the results.

Geometry optimization of **1a** and **1c** was performed without symmetry restrictions (under  $C_1$  point symmetry group). The bond lengths corresponded to the limiting case (for these systems) of  $D_{2h}$  symmetry to an accuracy of 0.015 Å. Geometry optimization of **1a** under  $D_{2h}$  symmetry and subsequent vibrational frequency calculations showed that this structure corresponds to a saddle point (one imaginary vibrational frequency of 50i cm<sup>–1</sup> was found). An imaginary frequency characterizes the vibrations accompanied by changes in the pseudotorsion angle C(1)—C(2)—C(9)—C(10) (angle  $\phi$ , see Fig. 1). It should be noted that in spite of imaginary frequency the energy difference between the **1a** anion structures with  $C_1$  and  $D_{2h}$  symmetry is only 0.1 kcal mol<sup>–1</sup>. This clearly indicates a flattened potential energy surface in the vicinity of the energy minimum for the torsional motion described above. A similar situation was also observed earlier in studies of neutral molecule **1**.<sup>18–20</sup> It was shown that symmetry of the structure corresponding to the energy minimum of **1** depends on the computational method and the basis set employed. For instance, B3LYP/4-21G(d) optimization of the structure with  $D_{2h}$  symmetry gave one imaginary frequency,<sup>18</sup> while MP2/6-31G calculations led to one and two imaginary frequencies for  $C_{2h}$  and  $D_{2h}$  symmetry, respectively.<sup>19</sup> Note that in the case of DFT calculations the results (e.g., imaginary frequencies) are affected by the numerical integration grid and by the type of convergence criteria. For instance, an appreciable de-

crease in the integration step in B3PW91/6-31G(d,p) calculations leads to positive values of all eigenfrequencies of the Hessian matrix. Hence, in this case the structure with  $D_{2h}$  symmetry can be treated as corresponding to an energy minimum.<sup>5</sup>

The results of calculations are in good agreement with the data of X-ray diffraction studies. Analysis of thermal motion in the crystal of compound **1** (space group  $P4_2/mnm$ ) showed that at 298 K the molecule is disordered due to the superposition of two  $D_2$  conformers differing in magnitude of the pseudotorsion angle  $\varphi$  ( $\varphi_1 = 3^\circ$ ,  $\varphi_2 = -3^\circ$ ).<sup>21</sup> A decrease in the temperature down to 100 K causes the freezing out of torsional motion and ordering of the molecule accompanied by an increase in the local symmetry to  $D_{2h}$ .<sup>5</sup>

For more correct analysis of redistribution of the electron density,  $\rho(\mathbf{r})$ , on going to the anion (**1a**) and cation (**1c**) the topological analysis was carried out ignoring the molecular symmetry.

Analysis of the geometry of the systems under study revealed that the main bond lengths in **1a** and **1c** are virtually the same as the corresponding parameters of molecule **1** (see Fig. 1, Table 2). The distance between the boat planes,  $d_2$ , depends on both the length of the ordinary bond C(1)—C(2) and the angle of deviation of the atom C(3). The  $d_2$  values for **1a** and **1c** are nearly the same (see Table 2), being smaller than for **1**. However, this shortening is due to different reasons, namely, the bond C(1)—C(2) in **1c** is 0.024 Å shorter than in **1** while the atom C(3) is characterized by greater deviation (0.191 Å vs. 0.159 Å in **1**). In **1a**, the bridging bond is somewhat less elongated (by 0.006 Å) while the deviation of the C(3) atom (0.131 Å) is smaller than in **1**.

The ring carbon—carbon bond lengths alternate. Depending on the charge of the species, the interatomic distance C(4)—C(5) changes to the greatest extent, being 0.012 Å shorter in **1c** and 0.027 Å longer in **1a** due to the

respective decrease and an increase in the electron density in the ring  $\pi$ -systems. Noteworthy is that the bond length variation similar to that found for **1a** is also observed for the metal-coordinated ring in those transition-metal complexes of **1** where molecule **1** acts as a  $\eta^6$ -ligand. For instance, according to X-ray diffraction study<sup>22</sup> of ( $\eta^6$ -[2.2]paracyclophane)chromium tricarbonyl, the distances C(3)—C(4) and C(4)—C(5) in the Cr-coordinated ring are 1.395 and 1.427 Å, respectively, and the C(1)—C(2) bond is lengthened to 1.599 Å as compared to the unsubstituted **1**. This is likely a case for  $\pi$ -electron back donation to the ligand aromatic system, which substantiates the possibility of using anion **1a** as a model for compounds with donor substituents.

The geometric parameters of the benzene anion and cation are in good agreement with the results of B3LYP/DZP++ calculations (see Refs. 15, 16). Similarly to **1a**, the benzene anion has a boat conformation with two carbons deviating from the ring plane by 0.13 Å. In contrast to system **1a**, the "central" bonds in the benzene anion are shortened to 1.390 Å (*cf.* 1.396 Å for benzene) while the remaining four bonds are lengthened to 1.425 Å. The benzene cation has a planar structure. The bond lengths in this system change in opposite directions compared to the benzene anion, namely, two oppositely lying bonds are lengthened to 1.451 Å while the remaining four bonds are shortened to 1.385 Å.

Analysis of the Mulliken spin densities in system **1a** showed that a negative charge of  $-0.2$  e is localized on the boat plane atoms and a charge of  $-0.12$  e is localized on the remaining ring atoms. In cation **1c**, four atoms (C(3), C(6), C(11), and C(14)) bear the most part of the positive charge (0.27 e). This is consistent with the behavior of neutral compound **1** in the electrophilic substitution reactions involving protonation at the C(3) atom.<sup>23</sup>

The charge distributions in **1a** and **1c** are in good agreement with the peculiarities of the electron localization function (ELF)<sup>24</sup> distribution shown in Fig. 2. The ELF characterizes the extent to which the kinetic energy density at a given point differs from the corresponding value calculated using the Thomas—Fermi approximation for free electron gas. The ELF values exceeding 0.5 correspond to the regions where the electron pairs and unpaired electrons are localized. The ELF values were calculated using the MORPHY program.<sup>25</sup> As can be seen in Fig. 2, the ELF sections in the regions of charge accumulation on the C(4) and C(5) atoms in systems **1c** and **1** (sections A1 and B1, respectively) obey a nearly identical pattern, whereas the electron density on these atoms in **1a** (section C1) appreciably increases with the distance from the center of the molecule. As to the systems **1a** and **1**, the electron density distributions on the atoms C(3) and C(14) also obey a nearly identical pattern (see Fig. 2, sections B2 and C2, respectively), while in system **1c** (section A2)

**Table 2.** Main geometric parameters of molecule **1**, radical anion **1a**, radical cation **1c**, benzene molecule, benzene radical anion, and benzene radical cation obtained from B3PW91/6-31+G(d) calculations

Bond, distance	Distance/Å					
	<b>1c</b>	<b>1</b>	<b>1a</b>	$C_6H_6^+$	$C_6H_6$	$C_6H_6^-$
C(1)—C(2)	1.580	1.604	1.598	—	—	—
C(2)—C(3)	1.513	1.510	1.509	—	—	—
C(3)—C(4)	1.418	1.400	1.400	1.390	1.396	1.425
C(4)—C(5)	1.380	1.392	1.419	1.451	1.396	1.385
C(3)...C(14)	2.661	2.805	2.781	—	—	—
C(4)...C(13)	3.044	3.121	3.043	—	—	—
$d^*$	0.191	0.159	0.131	—	—	—

\* Deviation of the C(3) atom from the C(4)—C(5)—C(7)—C(8) plane.

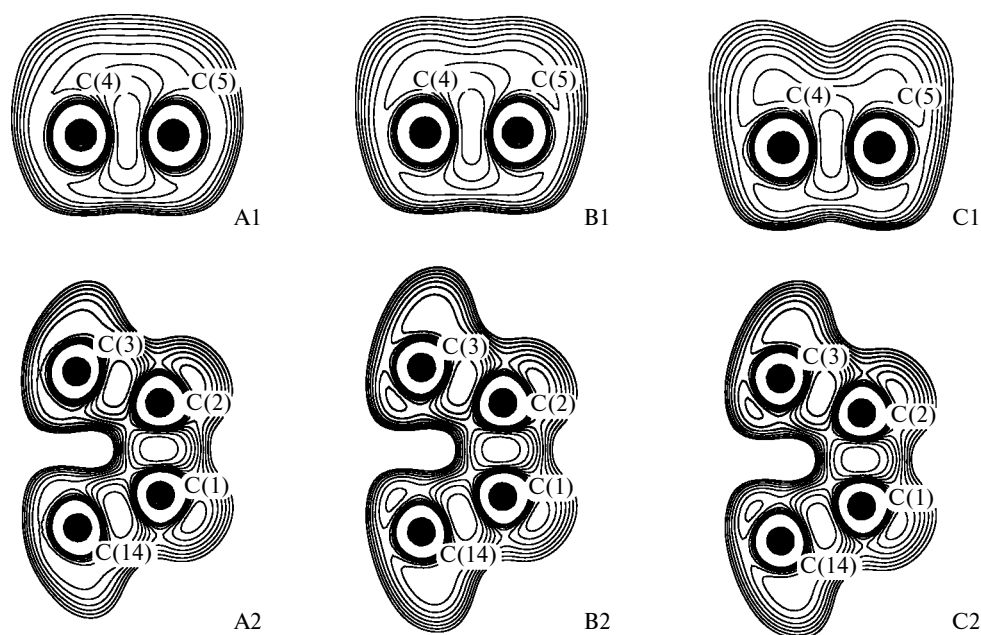


**Fig. 2.** Electron localization function (ELF) distribution in the region of the C(4)–C(5) bond and in the fragment C(3)–C(2)–C(1)–C(14) in cation **1c** (sections A1 and A2), molecule **1** (sections B1 and B2), and anion **1a** (sections C1 and C2) obtained from B3PW91/6-31+G(d) calculations. The contour plots correspond to the ELF values exceeding 0.5.

the maximum directed toward the center of the molecule is somewhat smaller.

The internal energy difference between the species **1a** and **1** corresponds to the electron affinity energy. It was estimated at 0.50 eV (B3PW91/6-31+G(d) calculations). The internal energy difference between **1** and **1c** corresponds to the first ionization potential. Here, our calculations gave a value of 7.45 eV, which is close to the experimental data (7.95 eV) obtained by UV photoelectron spectroscopy (see Table 1).<sup>25</sup> The calculated ionization potential and electron affinity energy of benzene are also consistent with the results of B3LYP/DZP++ calculations (see Refs. 15, 16).

In molecule **1**, charge delocalization over two aromatic systems occurs. Because of this, the first ionization potential and the electron affinity energy of **1** are lower than those of benzene. However, it should be noted that the relative decrease in the ionization potential is only 17% compared to benzene, whereas the electron affinity energy decreases by 63% (see Table 1).

The large (more than twofold) decrease in the electron affinity energy, the shortened (compared to neutral system **1**) interatomic distances C(3)–...C(14) and C(4)–...C(13), and a local increase in the atomic charges of C(3) and C(4) in **1c** and of the boat plane carbons in **1a** suggest the possibility of transannular interaction to occur in these systems. According to the AIM theory, such inter-ring interatomic interactions imply that the (3, –1) critical points (CPs) are located in the intramolecular space. However, topological analysis of the function  $\rho(\mathbf{r})$

carried out in this work showed that both systems **1** and **1c** are characterized by the same characteristic set of CPs including the (3, –1) CPs located in the regions of the carbon–carbon and C–H covalent bonds, the (3, +1) CPs corresponding to the formation of six-membered and twelve-membered rings, and the (3, +3) polyhedral CP. In the case of anion **1a**, the characteristic set of CPs additionally includes a group of four (3, –1) CPs located between the boat plane carbons and characterized by an electron density of  $0.085 \text{ e}\text{\AA}^{-3}$  (see Fig. 3) and four (3, +1) CPs corresponding to the formation of six-membered rings with  $\rho(\mathbf{r}) = 0.079 \text{ e}\text{\AA}^{-3}$ . Large separation (0.40 Å) between these CPs indicates stability of the characteristic

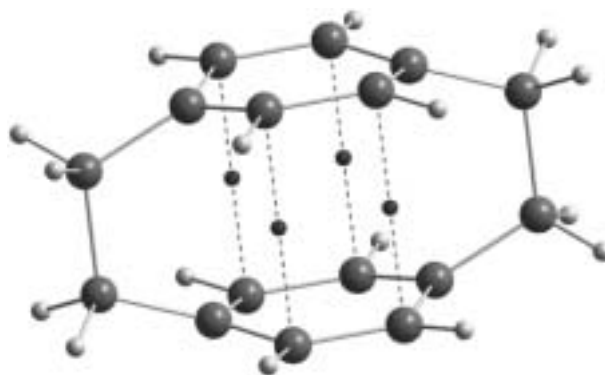


**Fig. 3.** General view of [2.2]paracyclophane radical anion; an illustration of the interaction between aromatic rings (dashed lines and small black circles in the interatomic space correspond to the bonding paths and to the (3, –1) CPs, respectively).

**Table 3.** Main topological characteristics of systems **1**, **1a**, and **1c** obtained from B3PW91/6-31+G(d) calculations

CP position	Parameter	<b>1c</b>	<b>1</b>	<b>1a</b>
Critical points (3, -1)				
C(1)—C(2)	$\rho(\mathbf{r})^a$	1.468	1.414	1.432
	$\nabla^2\rho(\mathbf{r})^b$	-10.46	-9.798	-10.03
	$\epsilon$	0.030	0.021	0.017
C(2)—C(3)	$\rho(\mathbf{r})$	1.700	1.705	1.706
	$\nabla^2\rho(\mathbf{r})$	-14.23	-14.16	-14.20
	$\epsilon$	0.001	0.028	0.027
C(3)—C(4)	$\rho(\mathbf{r})$	2.035	2.084	2.072
	$\nabla^2\rho(\mathbf{r})$	-19.59	-19.94	-19.58
	$\epsilon$	0.134	0.206	0.225
C(4)—C(5)	$\rho(\mathbf{r})$	2.157	2.090	1.980
	$\nabla^2\rho(\mathbf{r})$	-21.79	-20.03	-18.11
	$\epsilon$	0.134	0.222	0.198
C(5)—C(12)	$\rho(\mathbf{r})$	—	—	0.085
	$\nabla^2\rho(\mathbf{r})$	—	—	0.78
	$\epsilon$	—	—	1.23
Critical points (3, +1) and (3, +3)				
Six-membered ring	$\rho(\mathbf{r})$	0.139	0.143	0.139
	$\nabla^2\rho(\mathbf{r})$	4.00	4.06	3.79
	$ \lambda_1 ^b$	0.37	0.38	0.35
Twelve-membered ring	$\rho(\mathbf{r})$	0.068	0.059	0.060
	$\nabla^2\rho(\mathbf{r})$	0.77	0.64	0.77
Polyhedron	$\rho(\mathbf{r})$	0.030	0.024	0.028
	$\nabla^2\rho(\mathbf{r})$	0.50	0.45	0.45

<sup>a</sup> In  $\text{e} \cdot \text{\AA}^{-3}$  units.<sup>b</sup> In  $\text{e} \cdot \text{\AA}^{-5}$  units.

set of CPs<sup>8,26</sup> and its invariance with respect to both ring rotation and changes in the angle  $\phi$ . Indeed, calculations of system **1a** with a fixed value of the angle of rotation of the phenyl rings relative to each other ( $15^\circ$ ) showed that the characteristic set of CPs and the  $\rho(\mathbf{r})$  value in the region of transannular interaction remained unchanged.

Low electron density, as well as the positive signs of the electron density Laplacian and the electron energy density (0.009 a.u.), and high bond ellipticity (1.23) are characteristic of weak closed-shell interactions (see, e.g., Refs. 11, 12). Almost all interactions of this type (e.g., B...( $\pi$ -system),<sup>11</sup> S...S,<sup>12</sup> and halogen...halogen interactions<sup>27,28</sup>) can be described in terms of the "peak—hole" model. On the contrary, intramolecular interaction in the radical anion **1a** corresponds to the "peak—peak" type interaction and is similar in character to a recently described C=O...(triazole) contact in 2-(3-carboxamidofuroxan-4-yl)-4-nitro-5-carboxamido-2H-1,2,3-triazol-1-oxide.<sup>29</sup> This seems to be a common feature of the interaction between  $\pi$ -systems.

The eigenvalues,  $\lambda_1$ , of the Hessian matrix at the (3, +1) CPs of the phenyl ring characterize the curvature of the electron density distribution along the normal to the ring plane. Noteworthy is that their absolute values,  $|\lambda_1|$ , for **1a** and **1** are nearly equal (0.37 and 0.38  $\text{e} \cdot \text{\AA}^{-5}$ ) in

spite of the different charges of these systems (cf. a somewhat lesser value,  $|\lambda_1| = 0.35 \text{ e} \cdot \text{\AA}^{-5}$ , obtained for radical cation **1c**). The change in the absolute value of  $|\lambda_1|$  for these systems also shows that despite accumulation of the electron outside of the rings, in **1a** is also found an increase in the inter-ring space.

Those CPs that are common to all compounds studied in this work are characterized by close values of the main topological characteristics of the electron density distribution ( $\rho(\mathbf{r})$ ,  $\nabla^2\rho(\mathbf{r})$ , and bond ellipticity values). The largest difference was found for the (3, -1) CP in the region of the C(3)—C(4) bond ( $\rho(\mathbf{r}) = 2.16, 2.09$ , and  $1.98 \text{ e} \cdot \text{\AA}^{-3}$  for **1c**, **1**, and **1a**, respectively). The decrease in the electron density at this CP for **1a** is due to the inter-ring charge transfer.

Formally, the increase (decrease) in the ellipticity ( $\epsilon$ ) of the ordinary bond C(1)—C(2) in **1c** (**1a**) points to a respective decrease (increase) in the  $\pi$ -component of the bond and indirectly indicates an increase in the contribution of the inter-ring "through-the-ethylene-bridge" interaction. The C(3)—C(4) bond ellipticity correlates with the angle of deviation of the C(3) atom. For instance, the corresponding  $\epsilon$  value for **1a** is greater than for **1** because of the smaller angle of deviation in spite of the same C(3)—C(4) bond length (1.400 Å) in both systems.

Thus, our quantum-chemical study showed that the decrease in the electron affinity energy and stabilization of radical anion **1a** is a result of intramolecular transannular interaction. Taking into account a similar pattern of the bond length distribution in **1a** and transition metal complexes of **1**, we can hope that the transannular interaction also occurs in neutral molecules containing strong electron-donor groups, which is of unquestionable interest for creation of optoelectronic devices and materials possessing nonlinear optical properties.

This work was carried out with the financial support from the Russian Foundation for Basic Research (Project Nos. 03-03-32214 and 02-07-90169) and by the Russian Federation State Program of Support of the Leading Scientific Schools (Grant No. NSh 1060.2003.03) and Young Ph.D. Researchers (Grant No. MK-1209.2003.03).

## References

1. G. R. Desiraju and T. Steiner, *The Weak Hydrogen Bond in Structural Chemistry and Biology*, Oxford Science Publications, Oxford, 1999.
2. E. A. Meyer, R. K. Castellano, and F. Diederich, *Angew. Chem., Int. Ed. Engl.*, 2003, **42**, 1210.
3. C. Janiak, *J. Chem. Soc., Dalton Trans.*, 2000, 13885.
4. B. J. Holliday, F. P. Arnold, Jr., and C. A. Mirkin, *J. Chem. Phys. A*, 2003, **107**, 2737.
5. K. A. Lyssenko, M. Yu. Antipin, and D. Yu. Antonov, *Chem. Phys. Chem.*, 2003, **8**, 817.

6. R. F. W. Bader, *Atoms in Molecules. A Quantum Theory*, Clarendon Press, Oxford, 1990.
7. I. V. Fedyanin, K. A. Lyssenko, N. V. Vorontsova, V. I. Rozenberg, and M. Yu. Antipin, *Mendeleev Commun.*, 2003, 15.
8. S. Canuto, and M. C. Zerner, *J. Am. Chem. Soc.*, 1990, **112**, 2114.
9. (a) C. F. Matta, J. Hernández-Trujillo, T. Tang, and R. Bader, *Chem. Eur. J.*, 2003, **9**, 1940; (b) I. V. Glukhov, M. Yu. Antipin, and K. A. Lyssenko, *Eur. J. Inorg. Chem.*, 2004, **7**, 1379.
10. A. A. Korlyukov, K. A. Lyssenko, M. Yu. Antipin, V. N. Kirin, E. A. Chernyshev, and S. P. Knyazev, *Inorg. Chem.*, **41**, 2002, 5043.
11. W. Scherer, M. Spiegler, M. Tafipolsky, W. Hieringer, B. Reinhard, A. J. Downs, and G. S. McGrady, *Chem. Commun.*, 2000, 635.
12. K. A. Lyssenko, M. Yu. Antipin, M. E. Gurskii, Yu. N. Bubnov, A. L. Karionova, and R. Boese, *Chem. Phys. Lett.*, 2004, **384**, 40.
13. M. J. Frisch, G. W. Trucks, H. B. Schlegel, G. E. Scuseria, M. A. Robb, J. R. Cheeseman, V. G. Zakrzewski, J. A. Montgomery, Jr., R. E. Stratmann, J. C. Burant, S. Dapprich, J. M. Millam, A. D. Daniels, K. N. Kudin, M. C. Strain, O. Farkas, J. Tomasi, V. Barone, M. Cossi, R. Cammi, B. Mennucci, C. Pomelli, C. Adamo, S. Clifford, J. Ochterski, G. A. Petersson, P. Y. Ayala, Q. Cui, K. Morokuma, D. K. Malick, A. D. Rabuck, K. Raghavachari, J. B. Foresman, J. Cioslowski, J. V. Ortiz, A. G. Baboul, B. B. Stefanov, G. Liu, A. Liashenko, P. Piskorz, I. Komaromi, R. Gomperts, R. L. Martin, D. J. Fox, T. Keith, M. A. Al-Laham, C. Y. Peng, A. Nanayakkara, M. Challacombe, P. M. W. Gill, B. Johnson, W. Chen, M. W. Wong, J. L. Andres, C. Gonzalez, M. Head-Gordon, E. S. Replogle, and J. A. Pople, *GAUSSIAN-98, Revision A.7*, Gaussian, Inc., Pittsburgh (PA), 1998.
14. S. Pignataro and V. Mancini, *Chem. Commun.*, 1971, 142.
15. Y. Xie, H. F. Schaefer, III, and F. A. Cotton, *Chem. Commun.*, 2003, 102.
16. J. C. Rienstra-Kiracofe, C. S. Tschumper, H. F. Schaefer, N. Serela and G. B. Ellison, *Chem. Rev.*, 2002, **102**, 231.
17. J. Cheeseman, T. A. Keith, and R. W. F. Bader, *AIMPAC Program Package*, McMaster University, Hamilton (Ontario), 1992.
18. S. E. Walden and D. T. Glatzhofer, *J. Phys. Chem. A*, 1997, **101**, 8233.
19. D. Henseler and G. Honeicher, *J. Phys. Chem. A*, 1998, **102**, 10828.
20. D. Henseler and G. Honeicher, *J. Mol. Struct. (THEOCHEM)*, 2000, **497**, 145.
21. H. Hope, J. Bernstein, and K. N. Trueblood, *Acta Cryst.*, 1972, **B28**, 1733.
22. Y. Kai, N. Yasuoka, and N. Kasai, *Acta Cryst. Sect.*, 1978, **B34**, 2840.
23. F. Vögtle, *Cyclophane Chemistry. Synthesis, Structure and Reactions*, Wiley, Chichester New York, 1993.
24. A. Savin, R. Nesper, S. Wengert, and T. Fassler, *Angew. Chem., Int. Ed. Engl.*, 1997, **36**, 1809.
25. P. Popelier, *Chem. Phys. Lett.* 1994, **228**, 160.
26. J. Cioslowski and S. T. Mixon, *J. Am. Chem. Soc.*, 1992, **114**, 4382.
27. V. G. Tsirelson, P. F. Zou, T. H. Tang, and R. F. W. Bader, *Acta Cryst.*, 1995, **A51**, 143.
28. R. Boese, A. D. Boese, D. Blaser, M. Yu. Antipin, A. Ellern, and K. Seppelt, *Angew. Chem., Int. Ed. Engl.*, 1997, **36**, 1489.
29. I. V. Ovchinnikov, M. A. Epishina, S. I. Molotov, Yu. A. Strelenko, K. A. Lyssenko, and N. N. Makhova, *Mendeleev Commun.*, 2003, 272.

Received January 12, 2004